

HETGS observation of Cas A: Looking at the trees in the forest

J.S. Lazendic, D. Dewey, C.R. Canizares, and N.S. Schulz
MIT Kavli Institute, Cambridge MA, USA

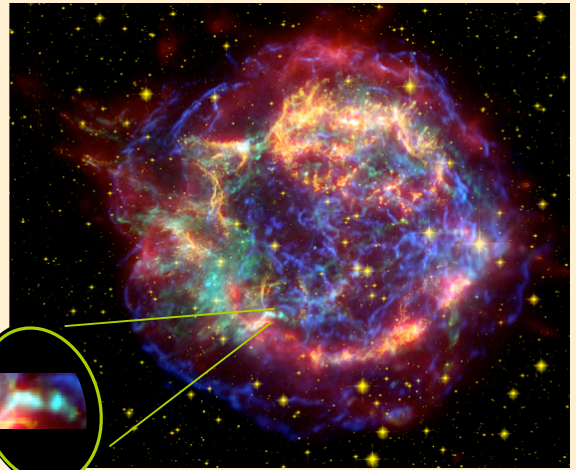
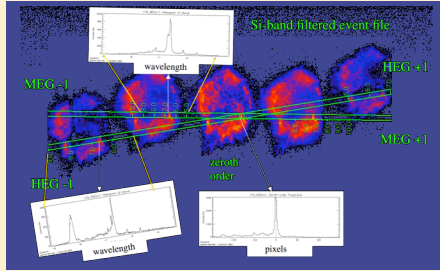


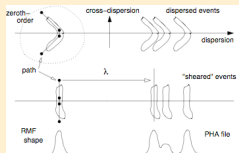
Image of Cassiopeia A combining observations from three of NASA's Great Observatories: The Chandra X-ray data is shown in green and blue (silicon line emission and 4-6 keV continuum, respectively), the Hubble optical image is in yellow, and the Spitzer infrared image is shown in red.
Credit: X-ray: NASA/CXC/SAO; Optical: NASA/STScI; Infrared: NASA/JPL-Caltech



HETGS image of Cas A filtered on the Si lines. The un-dispersed "zeroth-order" image is seen in the center with an example profile of a narrow, bright feature. To either side along the two grating dispersion axes, MEG and HEG, are seen dispersed images of the remnant in the Si lines. Precise measurement of the location of the dispersed features gives accurate Doppler velocity measurements and line flux information.

Introduction

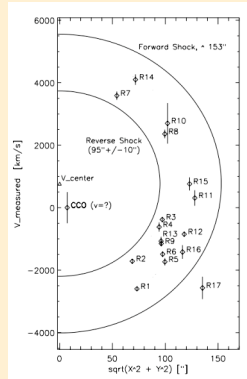
We present high-resolution X-ray spectral results from the young supernova remnant Cas A using a 70ks observation taken by the Chandra High-Energy Transmission Grating Spectrometer (HETGS). Line emission, dominated by Si and S, from many bright, narrow regions allows us to measure these regions' kinematic and plasma properties. With these high-resolution measurements we hope to advance the 3D modeling of Cas A begun by Markert et al. (1983) using the Einstein Focal Plane Crystal Spectrometer.



Simple schematic of the filament analysis. A "path" is defined on the zeroth-order and is used to narrow the projection of lines dispersed from the feature.

Filament Analysis

We used custom software (written in IDL) that basically follows the steps of the CIAO threads for grating spectra, but accounts for an extended, filament-like source when creating spectra (PHA files) and the corresponding instrument response files, RMFs, which relate photon wavelength to dispersion location. The resulting PHA, RMF, and a standard ARF file can then be used in, e.g., ISIS to carry out model fitting.



The 17 bright, narrow regions we studied are indicated **at right** on a silicon-line image of Cas A.

The plot **at left** has a data point for each of our regions indicating: measured velocity vs. the radial distance of the region from the optical expansion center. These points are seen to lie within a narrow shell in 3D between the reverse and forward shock locations (Gotthelf et al. 2001.) The one exception is R17 - is it part of the NE jet?!

Doppler-shift Results

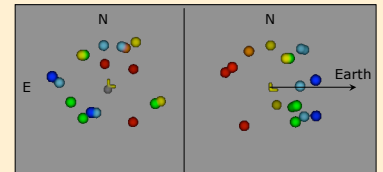
We derive Doppler shifts for these 17 regions, values range from a blue-shift of 2500 km/s to a red-shift of 4000 km/s. Combined with the spatial sky locations, these velocities are consistent with the Reed et al. (1995) velocity center of +770 km/s and an expansion rate of ~ 0.2 % per year (DeLaney & Rudnick 2003.) This eliminates an apparent "mismatch" of Doppler and transverse velocities (DeLaney et al. 2004) based on earlier X-ray results (Willingale et al. 2002.)

Color = Velocity

Key (km/s):
Red > +2500; Orange +2500 to +1000; Yellow +1000 to -500; Green -500 to -1300; Light-Blue -1300 to -2000; Blue < -2000

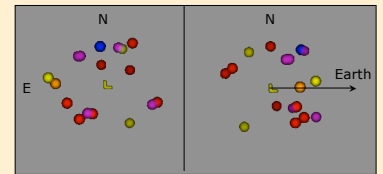
Using the velocities, the regions can be assigned a location along the line-of-sight adding a third-dimension. The region locations are shown here in "front" (Sky) view (**left**) and a "side" (3rdD) view (**right**.)

The Regions in 3D



Color = Temperature

Key:
Blue < 0.6 keV; Magenta 0.6-0.8 keV;
Red 0.8-1.4 keV; Orange 1.4-3.0 keV;
Yellow 3.0-5.0 keV

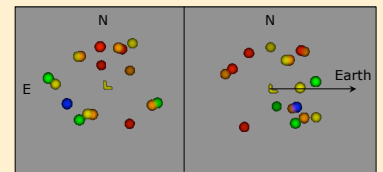


Color = t_{shock}

The time-since-shock-passage is given by:

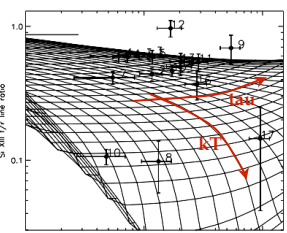
$t_{shock} = \tau / n_e$
The regions in the "back" of Cas A appear to be just recently shocked compared to most regions in the "front" which have longer t_{shock} 's.

Key:
Red < 30 yr.s; Orange 30-60 yr.s
Yellow 60-90 yr.s; Green 90-125 yr.s
Blue > 125 yr.s



Line Diagnostics

We use the high-resolution spectra from the HETGS to investigate the plasma state of the regions using line diagnostics. The forbidden to resonance line ratio, f/r , of the He-like triplet and the Si XIV to Si XIII line ratio are used (**at left**) to determine kT and τ ($= n_e t$) values for each region under the assumption of a simple NEI plasma model.

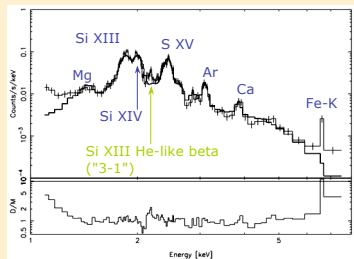


Location of the regions in Si ratio-ratio space, including an NEI kT-tau grid of model values.

Plasma Density

With each regions' kT and τ determined from the line ratios, we can determine the remaining parameters of a single VNEI model (Borkowski et al. 2001) by fitting the regions' non-dispersed zeroth-order spectra (**at left**.) Assuming an oxygen-rich plasma (Laming & Hwang 2003) and setting N_H to $1.5 \times 10^{22} \text{ cm}^{-2}$, we obtain reasonable fits in the Mg through Ca range.

We use the fit "norms" and abundances with the region volumes to determine plasma quantities for the regions: electron density, $n_e \sim 20$ to 200 cm^{-3} ; the time-since-shocked $t_{shock} = \tau / n_e \sim 10$ to 140 years; and the oxygen mass fraction ranging from 0.83 to 0.97.



The zeroth-order ACIS spectrum from region R9 with prominent Si XIV and Fe-K lines. The VNEI model curve has kT and tau fixed from the line ratio results.

Acknowledgments

We thank John Davis for contributions in the planning of the Cas A HETGS observation, and Glenn Allen, Mike Stage, Kathy Flanagan, Tracy DeLaney and Dan Patnaude for useful discussions. This work was supported by NASA through SAO contract SV3-73016 to MIT for Support of the Chandra X-Ray Center (CXC) and Science Instruments; the CXC is operated by the Smithsonian Astrophysical Observatory for and on behalf of NASA under contract NAS8-03060.

Contact: jasmina@space.mit.edu

References

- Borkowski, K.J. et al. 2001, ApJ, 548, 820.
- DeLaney, T. & Rudnick, L. 2003, ApJ, 589, 818.
- DeLaney, T., et al. 2004, ApJ, 613, 343.
- Gotthelf, E.V., et al. 2001, ApJ, 552, L39.
- Laming, J.M., & Hwang, U. 2003, ApJ, 597, 347.
- Lazendic, J., et al. 2006, in preparation.
- Markert, T.H., et al. 1983, ApJ, 268, 134.
- Reed, J.E., et al. 1995, ApJ, 440, 706.
- Willingale, R., et al. 2002, A&A, 381, 1039.